Dynamic triggering of earthquakes: the nonlinear slip-dependent friction case

Christophe Voisin

Dynamic triggering of earthquakes: The nonlinear slip-dependent friction case

C. Voisin[1]

Department of Geological Sciences, San Diego State University, San Diego, California, USA

Received 29 August 2001; revised 22 April 2002; accepted 7 May 2002; published 19 December 2002.

[1] The problem of earthquake triggering by dynamic stress waves is studied. A finite fault of length L embedded in an elastic space is considered. The prescribed nonlinear slip-dependent friction law is characterized by a nonconstant weakening rate α. The fault is perturbed by a sinusoidal stress wave of wavelength λ and amplitude a. As a general result, it is shown that for a given fault and a given friction law, low frequencies are more likely to trigger the rupture than high frequencies. In addition, the occurrence of triggering depends on the balance between intrinsic fault mechanics and the loading parameters. Two behaviors are possible depending on the friction law: some faults exhibit a threshold in frequency to be triggered, while other faults exhibit a threshold in amplitude. These two qualitative behaviors may be explained by considering the nondimensional weakening rate $\beta = \alpha \times L/2$ and β_0 the universal constant of stability computed by *Dascalu et al.* [2000]. The faults that present a threshold in frequency are intrinsically unstable: their initial nondimensional weakening rate $\beta(0)$ exceeds β_0. On the contrary, the faults that present a threshold in amplitude are intrinsically stable, i.e., initially $\beta(0) < \beta_0$. Because of the nonlinearity of the friction law, there is a characteristic slip u_c for which $\beta(u_c) \geq \beta_0$. For a sufficiently large amplitude the fault may then experience a stability/instability transition. These results are independent of the shape of the perturbation and also hold for a static stress increase. *INDEX TERMS:* 3220 Mathematical Geophysics: Nonlinear dynamics; 7209 Seismology: Earthquake dynamics and mechanics; 7260 Seismology: Theory and modeling; 3210 Mathematical Geophysics: Modeling

Citation: Voisin, C., Dynamic triggering of earthquakes: The nonlinear slip-dependent friction case, *J. Geophys. Res.*, *107*(B12), 2356, doi:10.1029/2001JB001121, 2002.

1. Introduction

[2] In the past 40 years it has been pointed out that earthquakes may interact. Earthquake interaction appears as a fundamental feature of seismicity, leading to earthquake sequences, clustering and aftershocks [*Stein*, 1999]. Since the pioneering work of [*Smith and Van de Lindt*, 1969], numerous studies have emphasized the role of static Coulomb stress transfer [*Harris*, 1998]. However, more and more studies exhibit seismicity patterns and fault behaviors that are not consistent with the Coulomb stress transfer theory: occurrence of triggered slip in stress shadows has been reported for many great Californian earthquakes [*Simpson et al.*, 1988] and recently for the Izmit earthquake [*Wright et al.*, 2001].

[3] During the propagation of the rupture front on a multisegmented fault it has been shown that dynamic stresses play a major role in the triggering of successive fault segments [*Harris and Day*, 1993; *Bouchon*, 1997]. It was demonstrated that even for longer delays between successive segment ruptures (as in the 1980 Irpinia earthquake where the delay was 20 s), the dynamic stresses play a significant role [*Voisin et al.*, 2000]. Dynamic triggering is found to be consistent with seismicity patterns [*Hill et al.*, 1993; *Anderson et al.*, 1994], especially for the Landers earthquake. Recently, *Kilb et al.* [2000] demonstrated a better correlation of the seismicity pattern following the Landers main shock with the dynamic peak stress of the Coulomb Failure Function. All these observations are inconsistent with static Coulomb stress transfer theory, which suggests that the dynamic stresses can play a role in determining the pattern of seismicity and rupture propagation.

[4] A limited number of studies exist that propose a physical model to explain why dynamic or transient stresses have an effect on fault behavior. One possible class of models consider the frictional properties of the fault and determine the possible effects of transient and permanent stresses on the nucleation process. *Gomberg et al.* [1998] considered a rate-and-state friction fault and developed a frictional instability model. The triggering stress perturbations included square wave transients and step functions, analogous to seismic waves and coseismic static stress. These perturbations were added to a constant background

[1]Now at Laboratoire de Geophysique Interne de Tectonophysique, Grenoble, France.

0148-0227/02/2001JB001121$09.00

stress-loading rate (tectonic load). The effects of these perturbations on the timing of the subsequent rupture have been discussed in the quasi-static approximation. The transition to the full dynamic analysis has not yet been studied. An alternative to rate-and-state friction is provided by slip-dependent friction laws [*Ohnaka et al.*, 1987]. *Voisin* [2001] used a finite fault under linear slip-dependent friction law to investigate the dynamic triggering of rupture. Using a sinusoidal plane wave, it was shown that the occurrence of triggering depends on the balance between the intrinsic mechanics of the fault and the loading characteristics. In this paper, I extend the first study to the more general case of a nonlinear friction law.

2. Model

[5] The finite difference scheme used in this study is described by *Ionescu and Campillo* [1999]. It was adapted to the case of a propagating stress wave by *Voisin et al.* [2000] and used by *Voisin* [2001].

2.1. Finite Fault

[6] A 2D antiplane finite fault of length L embedded in an elastic space is considered. The fault length is set to $L = 10$ km, a typical value for a fault segment. The shear wave velocity is $c = 3000$ m/s, the density of the medium is $\rho = 3000$ kg/m^3. The normal stress S_N is assumed to correspond to a depth of 5000 m.

2.2. Friction Law

[7] Following *Ionescu and Campillo* [1999], a nonlinear slip-dependent friction law with varying weakening rate is considered. The friction law is fully described by $\tau_s = \mu_s S_N$, $\tau_d = \mu_d S_N$, D_c, and a parameter $p \in [0, 1]$, respectively the static friction, the dynamic friction, the critical slip and a modulation factor. The friction law is nonlinear with respect to the slip displacement u and is given by the following relation:

$$\mu(u) = \mu_s - \frac{\mu_s - \mu_d}{D_c}\left\{u - (1-p)\frac{D_c}{2\pi}\sin(2\pi u/D_c)\right\} \quad (1)$$

It is interesting to consider also the derivative of friction with respect to the slip u since it has been shown by *Ionescu and Campillo* [1999] that $\mu'(0)$ greatly controls the slip rate evolution of the fault:

$$\mu'(u) = -\frac{\mu_s - \mu_d}{D_c}\{1 - (1-p)\cos(2\pi u/D_c)\} \quad (2)$$

This formulation is consistent with the previous study [*Voisin*, 2001] since the case $p = 1$ corresponds to the linear friction case (reference case). The case $p = 0$ corresponds to the other extreme case, for which we have the relation

$$\mu'(0) = 0 \quad (3)$$

[8] I choose $\mu_s - \mu_d = 0.08$, which corresponds to a stress drop $\Delta\tau \approx 11.5$ MPa. The friction decreases from τ_s to τ_d with the ongoing slip (initiation phase) until the slip reaches D_c on some part of the fault (Figure 1). The onset of rupture

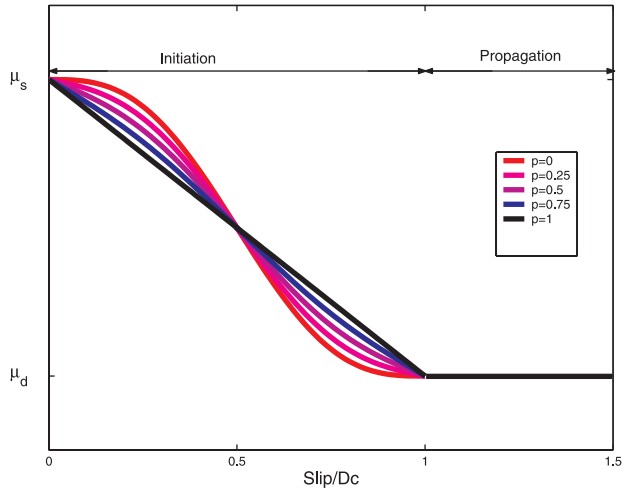

Figure 1. Nonlinear friction laws used in this study. The friction decreases from μ_s down to μ_d with the ongoing slip (initiation phase). As the slip reaches D_c, the friction stabilizes at the residual dynamic level (propagation phase). The parameter p allows for a change in the initial slope of the friction law.

(and the occurrence of triggering) corresponds to the end of the initiation phase and to a rupture propagation at the constant residual dynamic stress level. The initiation phase is characterized by the weakening rate α, given by the following relation:

$$\alpha(u) = \frac{-S_N}{G}\mu'(u), \quad (4)$$

where $G = \rho c^2$ is the rigidity modulus. Following *Dascalu et al.* [2000], I introduce the nondimensional weakening parameter $\beta(u)$ as:

$$\beta(u) = \alpha(u) \times \frac{L}{2}, \quad (5)$$

where L is the fault length. This nondimensional parameter completely characterizes the fault behavior. *Dascalu et al.* [2000] have performed a static stability analysis that reveals the intrinsic fault mechanics. They have computed the first nondimensional eigenvalue β_0 that determines the range of instability for the dynamic problem. This constant was found to be:

$$\beta_0 = 1.15777388\ldots \quad (6)$$

The fault behavior is governed by the relative magnitude of β and β_0. In case of $\beta < \beta_0$, the fault is stable, that is no slip or slip velocity instability can develop on the fault. In case of $\beta \geq \beta_0$, the fault is unstable and can be triggered. 5 different cases are considered in this study, depending on the value of the parameter p: the reference case ($p = 1$), and the cases $p = 0.75, 0.5, 0.25, 0$.

2.3. State of Stress

[9] The state of stress on the fault and in the medium is homogeneous and equals the static friction level τ_s. This

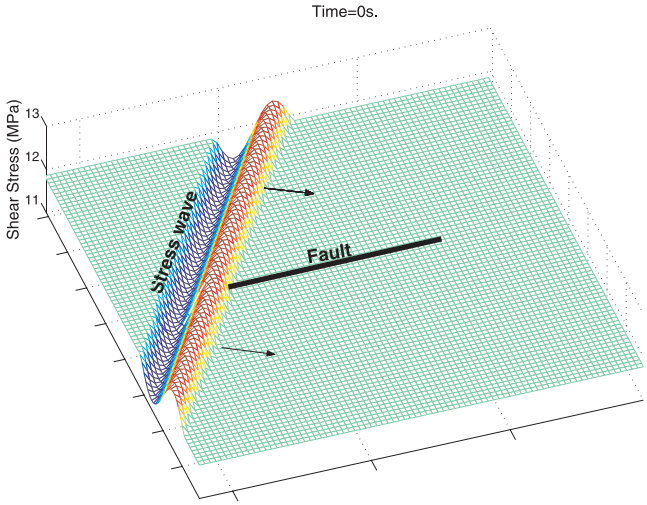

Figure 2. Geometry of the problem. At time $t = 0$ s the stress wave is just at one end of the fault. The black arrows indicate the direction of propagation. The medium shear stress equals τ_s. Red indicates stress greater than τ_s, while blue indicates stress lower than τ_s.

allows us to focus only on the effect of the stress wave, and not on the possible effect of prestress.

2.4. Incident Stress Wave

[10] The incident stress wave is a plane SH wave of sinusoidal shape. The wavelength λ and the amplitude a are both variable. The angle of incidence is set to $\theta = 45$ degrees. From the previous study [*Voisin*, 2001], it is clear that θ also plays a (limited) role on the occurrence of triggering since it modifies the duration of the loading on the fault. However, this effect will not be discussed in this study. At time $t = 0$ s the stress wave is exactly at one end of the fault (Figure 2).

3. Results

3.1. Linear Friction Case

[11] The linear friction case is extensively studied by *Voisin* [2001], but for the convenience of the reader, I recall here the main results. It is shown that the occurrence of triggering depends on the balance between the loading characteristics of the wave and the intrinsic fault mechanics. In this particular case, the wave's amplitude a exerts a clock advance effect: an increasing amplitude shortens the delay between the arrival of the wave and the start of rupture propagation. A limit frequency f_{lim} is defined which separates a triggering domain from a nontriggering domain. This limit depends on the slope of the friction law characterized by a nondimensional parameter β, constant all along the linear friction law.

3.2. Nonlinear Friction Case

[12] Figure 3 presents the computational results with the following notations: the wave's amplitude a is normalized to the stress drop $\Delta\tau = \tau_s - \tau_d$ and the wavelength λ to the fault length L. The numerical results presented here have been computed with $D_c = 1$ m and $L = 10$ km. Five different cases are considered, characterized by different values of p. The linear friction case ($p = 1$) serves as a reference. In such a case, it has been shown that the wave's amplitude a has no effect on the occurrence of triggering [*Voisin*, 2001]. It was stated that nonlinearity in the friction law will presumably make the wave's amplitude as important as the wave's frequency in the occurrence of triggering. This study confirms this hypothesis. The results in Figure 3 show that the wave's amplitude affects the fault behavior since the limits between triggering and nontriggering are no longer simple vertical lines. Thus the limit wavelength or frequency ($f_{lim} = c/\lambda$) is a function of the wave's amplitude a. In general, one can say that f_{lim} is an increasing function of the wave's amplitude a. This can be seen in Figure 3 since the limiting wavelength decreases as a increases. The study is confined to amplitude to stress drop ratio ranging between 0.01% and 50%. The lower bound is fixed by rounding errors. The upper bound is controlled by the loading exerted by the wave: a larger wave's amplitude will imply an amount of slip larger than the critical slip D_c on the fault.

[13] It is worth noting that two qualitatively different behaviors may be differentiated from Figure 3. The cases $p = 1$ (reference) and $p = 0.75$ exhibit the same type of behavior. The reference case exhibits a limiting wavelength ($\lambda/L = 0.39$) which separates a triggering domain (on the right) from a nontriggering domain on the left [*Voisin*, 2001]. The case $p = 0.75$ is slightly different from the reference case in that the wave's amplitude now affects the limiting wavelength. However, for small $a/\Delta\tau$ ratios lower than 1% the limiting wavelength seems quite independent from a. This corresponds to a limiting wavelength ratio λ/L

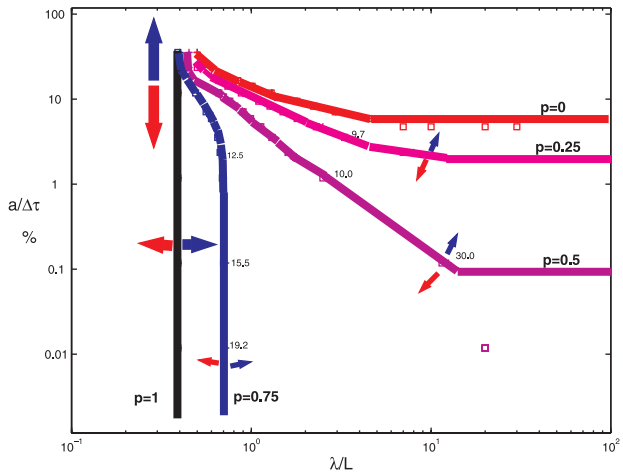

Figure 3. Results of the computation for a fault length $L = 10$ km and a critical slip $D_c = 1$ m. Depending on the wave's amplitude a, normalized to the stress drop $\Delta\tau$, and the wavelength λ, normalized to the fault length L, the fault is triggered (crosses) or not (squares). Each solid curve corresponds to a different value of p. Sensitivity of the triggering diagram to a change in the fault and friction parameters is also represented. Red arrows indicate a decrease in D_c or an increase in L; blue arrows indicate an increase in D_c or a decrease in L. The main effects are a shifting of the whole diagram leftward and downward in the first case and rightward and upward in the second case. Secondary effect concerns the rotation of the limits computed for $0 < p < 1$.

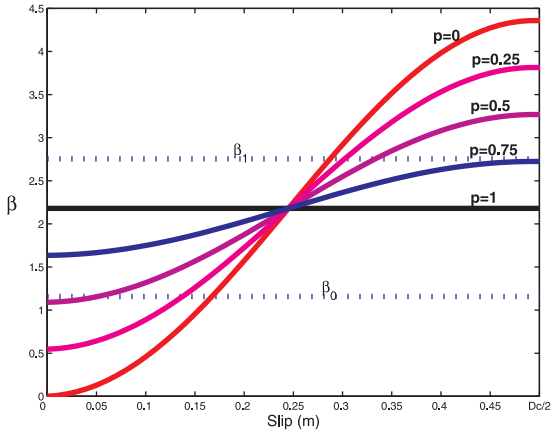

Figure 4. β as a function of slip, for the five different cases of the study. The static eigenvalues β_0 and β_1 have been plotted. Note that for $p = 0$, 0.25, and 0.5 the initial values of $\beta(u)$ are lower than β_0.

= 0.69. Therefore it is easier to define a threshold in the wave's frequency than in the wave's amplitude to trigger the fault under such friction laws. The cases $p = 0.5$, 0.25 and $p = 0$ exhibit another type of behavior. The wave's amplitude strongly affects the value of the limiting wavelength. Moreover for each of these cases there appears to be a minimum $a/\Delta\tau$ ratio under which it is difficult to trigger the fault. As will be shown later it is actually impossible to promote the rupture for amplitudes below this specific ratio. Consequently, a threshold in amplitude rather than a threshold in frequency is more adapted for such friction laws.

4. Interpretation

4.1. Two Behaviors, One Parameter

[14] Figure 4 presents the 5 different curves of $\beta(u)$, computed for a critical slip $D_c = 1$ m and a fault length $L = 10$ km. For the sake of comparison, the two first static eigenvalues β_0 and β_1 have been plotted on the same graph. These values mark the appearance of unstable modes for the fault [*Dascalu et al.*, 2000]. *Ionescu and Campillo* [1999] have shown the major role played by the initial slope of the friction on the slip rate evolution of the fault. Since the nondimensional weakening rate β is related to the slope of friction μ' by equations (4) and (5), it is interesting to focus on the initial values of β in the vicinity of $u = 0$. From Figure 4 one can see that for the cases $p = 1$ and $p = 0.75$ these initial values are greater than β_0. On the contrary, the case $p = 0.5$ and even more the cases $p = 0.25$ and $p = 0$ imply initial values of β lower than β_0.

[15] By analogy with the previous study [*Voisin*, 2001] and the work from *Dascalu et al.* [2000] the cases $p = 1$ and $p = 0.75$ correspond to intrinsically unstable friction laws. On the contrary, the cases $p = 0.5$, 0.25, 0 correspond to intrinsically stable friction laws and should not be triggered. However, since nonlinear friction law is considered, the nondimensional parameter β is a function of the amount of slip u, and for each friction law there exists a characteristic slip u_c for which $\beta \geq \beta_0$, so that the fault will experience a transition from stability to instability as the slip $u \geq u_c$ (see Appendix A).

[16] Depending on the loading parameters, the transition may or may not happen. Let us consider an incident stress wave of large amplitude. The loading is such that the amount of slip exceeds u_c: consequently the fault experiences a transition from stability to instability. On the contrary, an incident stress wave with small amplitude is unlikely to promote the transition, unless that the wavelength is dramatically increased. This can be seen in Figure 3 for the case $p = 0$. Large stress wave amplitudes (of the order of 20% of the stress drop) promote the transition from stability to instability and therefore it is possible to observe the triggering of the fault segment for relatively high frequencies. As the wave's amplitude decreases, the wavelength as to be dramatically increased in order to trigger the fault segment. This expresses the fact that a small amplitude must be compensated for by a large wavelength or equivalently by a low frequency. However, for a wave amplitude below a certain threshold it is physically impossible to trigger the rupture because the maximum slip imposed by the loading will remain lower than u_c, whatever the wavelength. Therefore the interpretation is straightforward: the two fault behaviors correspond to the two types of friction laws. Unstable friction laws lead to a threshold in the wave's frequency, whereas stable friction laws lead to a threshold in the wave's amplitude.

4.2. Influence of Fault and Friction Parameters

[17] The above results have been computed for a finite fault of length $L = 10$ km and a critical slip $D_c = 1$ m. The interpretation of these results presented in Figure 3 is entirely based on the role played by an unique nondimensional parameter β given by equation (5). The parameter β depends both on the fault length and the weakening parameter α, which in turn depends on the values of p and D_c. Do the present results remain valid if either the fault length L or the critical slip D_c are changed?

[18] Any change in any of the parameters will affect β through its total derivative:

$$d\beta = \frac{\partial\beta}{\partial D_c} dD_c + \frac{\partial\beta}{\partial L} dL + \frac{\partial\beta}{\partial p} dp + \frac{\partial\beta}{\partial\Delta\mu} d\Delta\mu \qquad (7)$$

Each of the terms composing $d\beta$ may be determined from equations (2)–(5) (see Appendix B). Let us consider first the linear friction case ($p = 1$), used as a reference (Figure 3). Any change in L or D_c will affect the value of β and move the position of this point. Any decrease in D_c or increase in L will increase β (red arrow). Any increase in D_c or decrease in L will decrease β and move the point toward the left (blue arrow).

[19] Let us now consider the nonlinear friction cases ($p \neq 1$). Since the wave's amplitude a may affect the triggering of the fault if the loading on the fault leads to an amount of slip exceeding the characteristic slip u_c, then the maximum wave's amplitude allowed must scale with u_c (and also with D_c). Thus, any change in the parameters that affect u_c will shift the whole triggering diagram vertically. However, since the characteristic slip u_c depends on D_c, L, p in a nonlinear way, it is not straightforward to determine how much the diagram will be affected by those changes. Finally, any change in D_c or L at constant p will affect β and consequently will move the triggering limits. A decrease

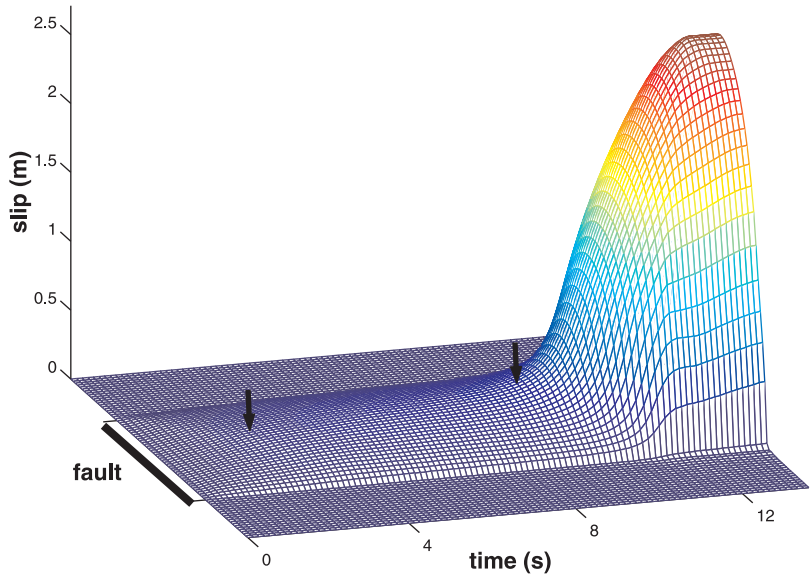

Figure 5. Slip response of a fault to a stress increase. The friction law corresponds to the case $p = 0$ presented in Figure 1. The first arrow (at time $t \approx 3$ s) marks the transition from stability to instability ($\beta = \beta_0$) when the slip equals the characteristic slip u_c. The slip then evolves in a nonlinear way until β becomes greater than β_1 (see Figure 4). This second transition is marked by the second arrow at time $t \approx 9$ s. At this moment the fault is far more unstable, and the slip dramatically increases.

in D_c or an increase in L (at constant p) will increase β. Consequently the triggering limit will be moved toward the instability, that is toward the linear case ($p = 1$). On the contrary, any increase in D_c or decrease in L at constant p will decrease β, and consequently move the triggering limit toward the stability, that is toward the case $p = 0$. It is interesting to note that neither the case $p = 1$ nor the case $p = 0$ are affected by these last changes.

5. Transition from Stability to Instability

[20] Many major and minor faults exhibit two behaviors, one is aseismic and is often associated with creep, the other is seismic and is associated with a sudden rupture episode. Evidences of these two behaviors have been documented in laboratory experiments as in the actual scale of faults [*Reinen*, 2000]. This implies the existence of transition from aseismic to seismic slip. *Iio* [1992], *Ellsworth and Beroza* [1995], and *Iio et al.* [1999] described a phase of slow, quasi-static slip prior to the onset of rupture. This phase was related to the nucleation process of the earthquake and was also observed in laboratory friction experiments [*Ohnaka*, 1996]. An aseismic fault movement before the 1995 Kobe earthquake has been detected by a GPS survey [*Zhao and Takemoto*, 1998].

[21] A key question for earthquake hazard assessment is what happens before these signals are detected? A possible answer has been suggested by *Dieterich* [1992] in the rate-and-state framework. I describe here a possible alternative model based on the slip-dependent friction law. To illustrate the role of the characteristic slip u_c and the stability of the first part of the friction law (when $\beta \leq \beta_0$) I perform two simulations. The loading is not a stress wave anymore but is rather a step stress increase, likely to represent a Coulomb shear stress increase. The friction law considered is the one given for $D_c = 1$ m, $p = 0$. The fault length is $L = 10$ km (Figure 1, case $p = 0$). At time $t = 0$ s, a stress increase is applied all over the medium. The response of the fault to this loading is shown in Figure 5. During the first few seconds, the fault slips stably to reach the new state of equilibrium imposed by the loading. The amount of slip soon reaches the characteristic slip u_c (first arrow). At this moment one can observe a change in the behavior of the slip evolution of the fault. Actually, as the slip reaches u_c, the nondimensional weakening parameter β exceeds β_0 and consequently the fault experiences a transition from stability to instability. The slip slowly increases in a nonlinear, exponential way. The instability growth rate can be evaluated by spectral methods [*Dascalu et al.*, 2000; *Voisin et al.*, 2002]. The nondimensional weakening parameter β is evolving with the slip, and eventually becomes greater than β_1 (the second static eigenvalue). This second transition is clearly visible in Figure 5 and corresponds to the sudden rapid increase in the slip evolution (second arrow). The end of the initiation phase is rapidly attained and the fault enters the rupture propagation stage as the slip reaches D_c. The second simulation considers the same fault and friction parameters. The static loading imposed at time $t = 0$ s is half the amplitude imposed in the previous simulation. This time, the loading is not strong enough to bring the fault to the slip u_c (Figure 6). The fault reaches a new stable equilibrium state corresponding to the new stress state. This last result first illustrates the stable character of the first part of the friction law. All points belonging to this first part are actual stable equilibrium positions for the fault. The immediate consequence of these results is that it exists a real threshold in the amplitude of the loading (stress wave or static stress increase). The lack of amplitude cannot be compensated for with a longer wavelength because the fault reaches a new equilibrium state. This means that under a

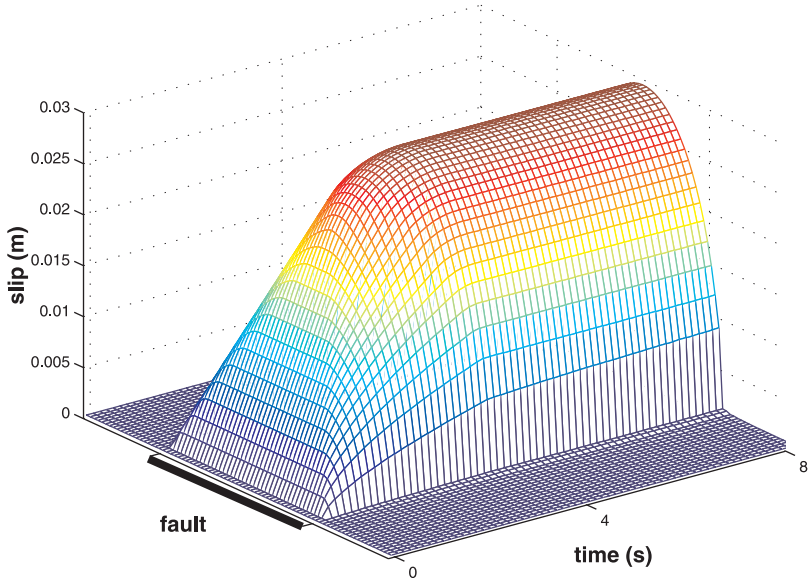

Figure 6. Slip response of the same fault to a small stress increase. The fault reaches the new equilibrium state imposed by the new state of stress. Note that the maximum of the slip amplitude of the new equilibrium state is lower than the characteristic slip u_c.

certain amplitude/stress drop ratio (to be determined: see Table A1) the fault cannot be triggered and remains in the stable part of the friction law.

6. Triggering of Earthquakes

6.1. Clock Advance Effect

[22] The results of the last section suggest that a transient wave or a static stress increase may enhance the likelihood of an impending earthquake on a fault which presents a stable friction law. Let us consider the case $p = 0$ presented in Figures 1 and 4. For such a friction law the characteristic slip u_c computed from equation (A3) is about 17 cm. The typical loading velocity for a fault, derived from GPS survey ranges between 1 cm up to 10 cm per year, while paleoseismological studies constrain the mean slip velocity about a few millimeters per year. Since the first part of the friction law is stable, the fault slip velocity in the slip-dependent model is totally controlled by external loading as long as the inertial terms are negligible. Therefore a fault that would obey such a friction law would need a time ranging between 1.7 up to 170 years to complete its stable part under tectonic loading once the critical stress level μ_s has been reached. Transient stress wave and static stress increase both hasten the time of occurrence of the next event by increasing temporarily or permanently the stress. The fault slips steadily until it reaches the new equilibrium state, or the unstable part of the friction law. A possible example of this behavior could be found in the Big Bear earthquake, apparently triggered 3 hours 26 min after the 1992 Landers earthquake. *King et al.* [1994] estimated the potential slip along the Big Bear fault to be about 60 mm to relieve the static stress increase due to the Landers earthquake. This represents about 5 to 10% of the subsequent final slip on this fault. Let us assume that the Big Bear fault obeys a slip-dependent friction law with both stable and unstable parts. Consider the potential slip of 6 cm has really occurred to relieve the static stress. According to the above presented results, the characteristic slip u_c for the Big Bear fault should be therefore at least 6 cm. The time delay of 3 hours 26 min may be due partly to the characteristic response time of the fault to the static stress increase. Figures 5 and 6 both show that the new equilibrium position is reached after a time delay. A part of the delay may be due also to the unstable initiation duration, which was proved to be extremely long as $\beta \approx \beta_0$, that is around the stable/unstable transition [*Voisin et al.*, 2002].

6.2. Triggering of Aftershocks

[23] *Kilb et al.* [2000] used the Landers earthquake wave train to estimate the optimal triggering threshold at a depth of 4.5 km (the mean depth of aftershocks). This threshold is about 0.1 MPa for the static stress and about 4.0 MPa for the dynamic stress waves. These authors hypothesized that large positive stress changes may significantly alter and weaken faults, enhancing their likelihood of failure, even if these large positive stress changes are only transient. However, this study lacks a physical model to explain why large transient waves may enhance the likelihood of failure more significantly than the static stress increase does. The model based on the slip-dependent friction law and transition from stability to instability offers a possible explanation. Considering that the stress drop of aftershocks ranges between 1 and 100 MPa, then the ratio wave's amplitude over stress drop lies between 4 and 400%. The ratio corresponding to the static threshold derived by *Kilb et al.* [2000] lies between 0.1 and 10%. The aftershocks occur on faults of smaller length, probably associated with lower values of the critical slip D_c. Therefore the triggering diagram (Figure 3) must be shifted upward and toward the right because of the size effect. A fault length of $L = 1$ km will shift the whole diagram upward by at least one decade. Simple consider-

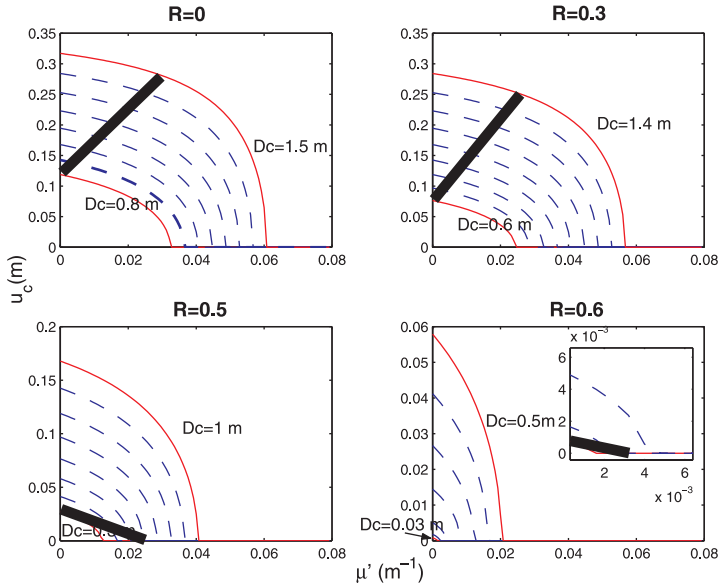

Figure 7. Value of the characteristic slip u_c for the 20 s fault segment of the Irpinia (Italy) earthquake. Here u_c is derived from the values of D_c and $\mu'(0)$ computed by *Voisin et al.* [2000]. R represents the prestress. In most of the cases u_c is greater than zero, which indicates that the 20 s fault segment was stable at the onset of its own rupture.

ations allow us to use the triggering diagram also for static stress perturbations. First, all faults under an unstable friction law ($p = 1$ or $p = 0.75$) will be triggered by a static stress perturbation. Unstable faults do not have any triggering threshold while perturbed by a static stress field. Second, the faults that have a stable part have an amplitude threshold. As shown in Figures 5 and 6 this amplitude threshold remains valid when using a static stress step. Consequently, the triggering diagram for a static stress step would be very simple: it would be formed of the three amplitude thresholds corresponding to the three stable cases ($p = 0$, 0.25, and 0.5). The reader is advised that these considerations are valid only on short timescales. Long term deformation processes such as plastic deformations are not taken into account in this study and may seriously affect the triggering threshold.

[24] Keeping in mind the ratios derived by *Kilb et al.* [2000] one can understand that the static stress trigger faults that are unstable or really close to instability. On the contrary the dynamic waves with larger amplitude are able to trigger both stable and unstable faults. *Hardebeck et al.* [1998] have demonstrated the absence of correlation of the seismicity with the static Coulomb stress increase when this increase is lower than 0.05 MPa. On the contrary, if the stress increase is greater than 0.1 MPa, a positive correlation is observed. According to the model of transition from stability to instability, this signifies that a 0.05 MPa increase in the static stress is not sufficient to promote the instability. Considering the same range for the stress drop, 1–100 MPa, the ratio amplitude/stress drop lies between 5.10^{-2}–5.10^{-4}. From Figure 3, it is clear that a stress step with such a low ratio would trigger only unstable faults (the cases $p = 1$ and 0.75), while a dynamic stress wave with a 4% ratio would trigger the cases $p = 1$ and 0.75 (unstable) as well as the cases $p =$ 0.5 and 0.25 (stable), depending on the frequency. Only the case $p = 0$ would not be affected by such a wave.

6.3. Multisegmented Rupture

[25] Perhaps the clearest evidence of dynamic triggering of a multisegmented rupture has been provided by the 1992 Landers earthquake. *Bouchon et al.* [1998] calculated the stress history all along the fault from the tomographic image of slip obtained by *Cotton and Campillo* [1995]. According to these calculations, an increase of 20–30 MPa in the shear stress was required to start the sliding on the Emerson fault. This large stress buildup generated by the rupture of the adjacent fault segments was necessary to overcome the lower tectonic shear stress and the higher friction (due to the higher normal stress) on the Emerson-Camp Rock fault segment. Assuming a 30 km length for this segment, and an average stress drop of 20 MPa [*Bouchon et al.*, 1998], it is possible to derive a constrain on the stable or unstable character of the segment at the onset of the rupture with the transition model. The critical slip D_c for the Emerson-Camp Rock fault segment has been estimated from the radiated seismic energy and the apparent stress by *Pulido and Irikura* [2000] to equal about 1 m. Equation (A3) allows the computation of the characteristic slip as a function of the parameter p. It appears that for these particular values of D_c,L and stress drop, the characteristic slip u_c ranges between 0 and 0.07 m. From Figure 3 one can understand that a fault length $L = 30$ km shifts the diagram downward and toward the left. The 20–30 MPa stress buildup leads to a wave's amplitude/stress drop ratio of 1–1.5. Therefore it is clear that such a wave will have triggered even the most stable fault (obtained for $p = 0$ and $u_c = 0.07$ m). In other words it is not possible to discriminate whether the Emerson-Camp Rock fault segment at the onset of its rupture was either stable or unstable.

[26] Another case of multisegmented rupture is provided by the 1980 Irpinia, Italy, earthquake sequence. This earthquake is composed of three subevents each separated in time by nearly 20 s. *Belardinelli et al.* [1999] and *Voisin et al.* [2000] have investigated the triggering of the second subevent by the main shock. Taking into account the travel time propagation between the two segments, a delay of nearly 18 s remains between the time of the wave arrival on the second segment and the onset of its rupture. *Belardinelli et al.* [1999] explained this delay in terms of a frictional instability, using a rate-and-state dependent friction law. *Voisin et al.* [2000] explained the 18 s delay in term of a nucleation process triggered by the passage of the dynamic waves generated by the main shock. It was demonstrated that the dynamic pulse by itself was sufficient to explain the triggering of the second subevent. An interesting question to answer is the following: can we infer from these parameters if the second fault segment was stable or unstable at the onset of its own rupture? For four choices of $R = \sigma - \tau_0$ (fault strength minus initial shear stress) it was possible to determine the couples of parameters ($\mu'(0)$, D_c) that lead to the 18 s delay. From these couples, and assuming fixed values for the fault length and the stress drop, it is easy to derive the dependence of the characteristic slip u_c with μ' for each value of D_c. This is achieved in Figure 7. The thick black line in each subplot represents the value of the characteristic slip u_c which corresponds to each couple ($\mu'(0)$, D_c) that leads to the observed delay of 18 s. For instance, let us consider the case $R = 0$ MPa, that is a fault close to failure (the initial stress level equals the yield strength). In such a case the parameters leading to the 18 s delay were found to range between 0.8 and 1.5 m for D_c, and 0 to 0.03 m^{-1} for $\mu'(0)$ [*Voisin et al.*, 2000]. For each value of D_c the value of $\mu'(0)$ is known, from which the corresponding value of u_c is derived. In the case $R = 0$ the characteristic slip u_c ranges from 0.1 m up to 0.27 m. This implies that for each couple the characteristic slip u_c is strictly greater than 0, which in turn implies that all the friction laws leading to the 18 s delay present a stable part. The same conclusion is reached for the case $R = 0.3$ MPa. The cases $R = 0.5$ and 0.6 MPa are slightly different. For the case $R = 0.5$ MPa the thick black line does not span the range of possible values of D_c but rather stops for $D_c = 0.6$ m. This signifies that for $D_c > 0.6$ m, $u_c = 0$ and the friction laws leading to the 18 s delay correspond to unstable faults. For the case $R = 0.6$ MPa, $u_c = 0$ as $D_c > 0.05$ m. That is most of the friction laws leading to the 18 s delay are unstable. This analysis suggests that both states, stable or unstable, are possible with a high prestress (low values of R) implying a stable fault, and low prestress (greater values of R) an unstable fault.

7. Discussion

7.1. Effect of the Prestress

[27] Up to now, only the case $\tau_i = \tau_s$ has been considered. Under such a condition the fault may evolve freely. However, it seems that the actual stress level throughout the upper crust does not equal the yield strength of the faults, but is lower. The ratio τ_i/τ_s defines the prestress. It is obvious that the prestress will quantitatively affect the results presented in this study. The first and immediate effect will be to shift upward the whole diagram in Figure 3, which means that the amplitude of the incident wave must be increased to overcome the prestress. The second effect is less immediate. The duration of the loading, defined as the total amount of time during which the stress level on the fault is greater or equal to the yield strength, is also a function of the prestress. As the prestress tends toward 1, the duration of the loading is directly related to the wavelength of the sine wave. If the prestress is lower than 1, the duration of the loading is decreased. According to the results presented above, a given fault is less sensitive to a short wavelength than to a large one. Therefore, the effect of prestress is to stabilize the fault. If the incident stress wave has an amplitude too small to reach the yield strength of the fault, this latter will remain unabated.

7.2. Effect of a Seismogram

[28] So far, only a simple sine wave has been considered without any variation of the normal stress. The wave train formed by an earthquake is composed of different types of waves which have several effects. First, the total duration of loading is increased which promotes triggering. Second the normal stress may be alternatively increased and decreased, which changes the yield strength on the fault. The decrease in the yield strength may be substantial enough to promote the triggering of understressed faults by simply equating τ_s and τ_i (unclamping of the fault). According to the model presented above, the low frequencies and large amplitude are more likely to trigger the rupture than small amplitude and high frequencies. Surface waves are then the most effective waves for the occurrence of triggering, as it was observed after the Landers earthquake [*Gomberg and Bodin*, 1994].

7.3. Tidal Triggering of Earthquakes

[29] Tidal stress waves are extremely low frequency (periods of 12.5 hours and 14 days), and accordingly to the model should favorize the triggering of events despite of their small amplitude ranging between 0.001 and 0.004 MPa [*Melchior*, 1983; *Vidale et al.*, 1998]. Recent studies about tidal triggering have focused on the existence of a possible correlation between the peak of the tidal forcing and the peak of seismicity: *Lockner and Beeler* [1999] have investigated through laboratory experiments the tidal triggering of earthquakes. They showed two principal results: the first is the presence of premonitory slip prior to the stick-slip event. The second is the existence of a threshold in stress level that separates a strongly correlated regime from a poorly correlated regime. The transition between these two regimes is for amplitudes between 0.05 and 0.1 MPa. Therefore the small amplitude of tidal stress waves does not permit a strong correlation between the peak shear stress and the seismicity, whereas the large amplitudes created by the 1992 Landers earthquake (greater than 0.1 MPa) in a broad range of frequencies lead to a strongly correlated regime. Obviously, if the faults in the upper crust were even slightly understressed, the small oscillations of the tides will be totally inefficient and will not affect the faults. On the contrary, if the stress on the fault equals the yield strength, then one can derive a constrain on the characteristic slip of actual faults from the absence of correlation with the Earth tides. The largest amplitude of the tides is about 0.004 MPa, which

implies a characteristic slip u_c of the order of a few millimeters.

7.4. Effect of the Shape of the Friction Law

[30] Throughout this study, I have used a nonlinear slip-weakening friction law. This is motivated by the laboratory experiments that have shown the relevance of a slip-dependent friction law to stick-slip dynamics [*Ohnaka et al.*, 1987]. *Campillo and Ionescu* [1997] and *Ionescu and Campillo* [1999] have studied the nucleation process under slip-dependent friction. They have shown that the duration of nucleation is related to both fault and friction characteristics. *Dascalu et al.* [2000] have revealed the existence of β_0, a threshold in the fault stability. The nondimensional weakening parameter β must be greater than β_0 to insure the existence of the unstable nucleation process. All these results and those of this study were obtained for slip-weakening friction. However, *Ohnaka and Yamashita* [1989] have shown that the slip-dependent friction law presents a slip-strengthening part at the beginning. This strengthening part may alter the results presented in Figure 3 quantitatively, but not qualitatively. As a matter of fact, the transition from stability to instability is obtained as $\beta > \beta_0$, and not when $\beta > 0$ (the sign convention is positive for weakening, negative for strengthening). Therefore, as long as $\beta < \beta_0$ as it is the case during slip strengthening, the fault remains stable. If the qualitative behavior is unchanged, the quantitative results may be way different, as slip strengthening will affect the wave's characteristics able to trigger the rupture. For instance, the wave's amplitude a will have to be much larger to overcome the slip-strengthening part and force the fault to the slip-weakening part. This implies a whole upward shift of the triggering diagram presented in Figure 3.

7.5. Effect of Small-Scale Heterogeneities

[31] The present study considered a finite homogeneous fault as well as a smooth friction law. However, small-scale heterogeneities along the fault surface can affect the shape of the friction law by introducing high-frequency bumps and lows. *Campillo et al.* [2001] and *Voisin et al.* [2002] have investigated the effects of small scale heterogeneities of friction properties on the nucleation process. The major effect is to extend the initiation duration. *Voisin et al.* [2002] have developed the concept of spectral equivalence between the heterogeneous fault and a homogeneous fault associated with a lower β. *Campillo et al.* [2001] have shown that the homogeneous equivalent fault is associated with an equivalent nonlinear slip-dependent friction law characterized by a smaller initial slope (which explains why the initiation duration is extended). The equivalent friction law reproduces the global features of the heterogeneous nucleation process, but evidently loses the details due to the heterogeneities. So far, only simple periodic fluctuations of frictional properties have been considered [*Campillo et al.*, 2001; *Voisin et al.*, 2002]. Much more work has to be done for more complex cases such as random fluctuations to determine the conditions of existence of an equivalent friction law. It is possible that the slippage of local heterogeneities may be promoted by a wave whose frequency is too high to promote the triggering of the whole fault segment, possibly leading to local micro-events on the fault. The possibility than one of these micro-events grows and eventually spans the entire fault plane cannot be ruled out, except if the fault heterogeneities may be represented by an equivalent friction law. Therefore, the finite homogeneous fault with slip-weakening friction used in the present study must be understood as representing the global behavior of an heterogeneous fault.

8. Conclusions

[32] The dynamic triggering of earthquakes is studied for the case of a finite fault under a nonlinear slip-dependent friction law. It is found that both the wave's frequency and amplitude affect the potential for triggering. Large amplitude and low frequency waves are more likely to trigger the rupture than small amplitude and high frequency waves. Two qualitatively different behaviors are possible. Some faults exhibit a frequency threshold, while some other faults exhibit an amplitude threshold. As stated by *Voisin* [2001] the occurrence of triggering depends on the balance between the intrinsic mechanics of the fault and the loading characteristics, and the two behaviors can be explained in the same framework. Considering the nondimensional weakening rate $\beta = \alpha \times L/2$ and β_0 the universal constant of stability computed by *Dascalu et al.* [2000], it appears that the two behaviors correspond to two types of friction laws. Faults which present a frequency threshold are intrinsically unstable ($\beta(0) > \beta_0$). Faults which present a threshold in amplitude are intrinsically stable, that is, initially $\beta(0) < \beta_0$. For certain parameter values, and because of the nonlinearity of the friction law, there exists a characteristic slip u_c for which $\beta(u_c) \geq \beta_0$ implying a transition from stability to instability. *Voisin et al.* [2000] studied the 1980 Irpinia (Italy) sequence. Focusing on the triggering of the second subevent 18 s after the main shock, it has been possible to derive the friction parameters (D_c, $\mu'(0)$) that lead to this delay. These results are used here to derive the characteristic slip u_c as a function of the prestress. It is shown that for most of the couples (D_c, μ') the characteristic slip ranges between 0.1 and 0.3 m, so that the fault is stable. A trade-off between prestress and fault stability is observed: high prestress is consistent with a stable fault, while low prestress is more consistent with an unstable fault. Concerning aftershocks triggering, the lack of correlation with the static stress increase under 0.1 MPa may indicate the existence of either a low regional prestress and/or the existence of a stable part of the friction law. The transition model offers a new model of faulting evolution that will be investigated in future research..

Appendix A: Characteristic Slip u_c

[33] From equations (2)–(5) one can obtain:

$$\beta = \frac{S_N}{G} \times \frac{\mu_s - \mu_d}{D_c} \left\{ 1 - (1-p) \cos\left(\frac{2\pi u}{D_c} \right) \right\} \times \frac{L}{2} \qquad \text{(A1)}$$

The characteristic slip u_c is defined as follows:

$$u_c : u_c \in [0; D_c] \text{ such that } \beta(u_c) = \beta_0 \qquad \text{(A2)}$$

From equations (A1) and (A2) it becomes

$$u_c = \frac{D_c}{2\pi} \arccos\left\{ \frac{1}{1-p} \left(1 - \frac{2\beta_0 G D_c}{S_N(\mu_s - \mu_d)L} \right) \right\} \qquad \text{(A3)}$$

Table A1. Minimum Amplitude/Stress Drop Ratio to Promote the Triggering of a Stable Fault as a Function of p[a]

	Value of p						
	0	0.1	0.20	0.25	0.3	0.4	0.5
u_c	0.172	0.163	0.153	0.1425	0.133	0.107	0.056
Minimum ratio, %	4.67			2.0			0.1

[a]Values are computed for D_c = 1 m and L = 10 km.

u_c is not defined for $p = 1$, that is for the linear case. This is quite obvious since in the linear case β does not depend on the slip and is either lower or greater than β_0 without any change. That is a linear friction law is always stable or always unstable [*Voisin*, 2001]. A second limit to the definition of u_c comes from the argument of the function inverse cosine. The absolute value of this argument has to be lower than 1.

$$\left|\frac{1}{1-p}\left(1-\frac{2\beta_0 GD_c}{S_N(\mu_s-\mu_d)L}\right)\right| \le 1 \tag{A4}$$

which after some algebra gives

$$1 > \frac{2\beta_0 GD_c}{S_N(\mu_s-\mu_d)L} \ge p \tag{A5}$$

Equation (A5) provides a relation between the different fault and friction parameters of the model to insure the existence of the characteristic slip u_c and therefore the possibility of a transition from stability to instability. The major role played by the stable part of the friction law and the characteristic slip u_c has been emphasized in section 5. In order to demonstrate that only the amplitude is important here, the transient stress wave has been replaced by a static shear stress increase. Table A1 summarizes the minimum amplitude needed to compel the fault to completely describe the stable part of friction and to be eventually triggered.

Appendix B: Derivatives of β With Respect to the Fault and Friction Parameters

[34] The total derivative of β is given by equation (7). After some algebra one can obtain the following partial derivatives of β with respect to the fault and friction parameters:

$$\frac{\partial\beta}{\partial D_c} = -\frac{\Delta\mu}{D_c^2}\frac{S_N L}{G}\left\{1-(1-p)\cos\frac{2\pi u}{D_c}-\frac{\pi}{D_c}(1-p)u.\sin\frac{2\pi u}{D_c}\right\} \tag{B1}$$

$$\frac{\partial\beta}{\partial p} = \frac{\Delta\mu}{2D_c}\cos\frac{2\pi u}{D_c}\times\frac{S_N L}{G} \tag{B2}$$

$$\frac{\partial\beta}{\partial L} = \frac{\Delta\mu}{2D_c}\left\{1-(1-p)\cos\frac{2\pi u}{D_c}\right\}\frac{S_N}{G} \tag{B3}$$

$$\frac{\partial\beta}{\partial(\Delta\mu)} = \frac{1}{2D_c}\left\{1-(1-p)\cos\frac{2\pi u}{D_c}\right\}\frac{S_N L}{G} \tag{B4}$$

Since the initial value of β is prominent in the fault behavior, let us place in the vicinity of $u = 0$. The sign of the partial derivatives of β gives us the sensitivity of β with respect to the parameters. It is obvious that $\partial\beta/\partial D_c$ is the only non positive derivative. That is an increase in D_c will decrease the value of $\beta(0)$, enhancing the stability of the fault. On the contrary, since all the others derivatives are positive any increase in p, L or $\Delta\mu$ will increase $\beta(0)$ and enhance the instability of the fault.

[35] **Acknowledgments.** I would like to thank F. Cotton, I. Ionescu, J. Gomberg, and T. Yamashita for their careful reviews. This paper is dedicated to Morgane, for her support.

References

Anderson, J., J. Brune, J. Louie, Y. Zeng, M. Savage, G. Yu, Q. Chen, and D. dePolo, Seismicity in the western great basin apparently triggered by the Landers, California, earthquake, 28 June 1992, *Bull. Seismol. Soc. Am.*, *84*, 863–891, 1994.

Belardinelli, M. E., M. Cocco, O. Coutant, and F. Cotton, Redistribution of dynamic stress during coseismic ruptures: Evidence for fault interaction and earthquake triggering, *J. Geophys. Res.*, *104*, 14,925–14,945, 1999.

Bouchon, M., The state of stress on some faults of the San Andreas System as inferred from near-field strong motion data, *J. Geophys. Res.*, *102*, 11,731–11,744, 1997.

Bouchon, M., M. Campillo, and F. Cotton, Stress field associated with the rupture of the 1992 Landers, California, earthquake and its implications concerning the fault strength at the onset of the earthquake, *J. Geophys. Res.*, *103*, 21,091–21,097, 1998.

Campillo, M., and I. Ionescu, Initiation of antiplane shear instability under slip-dependent friction, *J. Geophys. Res.*, *102*, 20,363–20,371, 1997.

Campillo, M., P. Favreau, I. Ionescu, and C. Voisin, On the effective friction law of an heterogeneous fault, *J. Geophys. Res.*, *106*, 16,237–16,250, 2001.

Cotton, F., and M. Campillo, Inversion of strong ground motion in the frequency domain: Application to the 1992 Landers, California earthquake, *J. Geophys. Res.*, *100*, 3961–3975, 1995.

Dascalu, C., I. Ionescu, and M. Campillo, Fault finiteness and initiation of dynamic shear instability, *Earth Planet. Sci. Lett.*, *177*, 163–176, 2000.

Dieterich, J., Earthquake nucleation on faults with rate-and-state dependent strength, *Tectonophysics*, *211*, 115–134, 1992.

Ellsworth, W., and G. Beroza, Seismic evidence for an earthquake nucleation phase, *Science*, *268*, 851–854, 1995.

Gomberg, J., and P. Bodin, Triggering of the m_s = 5.4 Little Skull Mountain, Nevada, earthquake with dynamic strain, *Bull. Seismol. Soc. Am.*, *84*, 844–853, 1994.

Gomberg, J., N. Beeler, M. Blanpied, and P. Bodin, Earthquake triggering by transient and static deformations, *J. Geophys. Res.*, *103*, 24,411–24,426, 1998.

Hardebeck, J., J. Nazareth, and E. Haucksson, The static stress change triggering model: Constraints from two southern California aftershocks sequences, *J. Geophys. Res.*, *103*, 24,427–24,438, 1998.

Harris, R., Stress triggers, stress shadows, and implications for seismic hazard, *J. Geophys. Res.*, *103*, 24,347–24,358, 1998.

Harris, R., and S. Day, Dynamics of fault interaction: Parallel strike-slip faults, *J. Geophys. Res.*, *98*, 4461–4472, 1993.

Hill, D., P. Reasenberg, A. Michael, W. Arabaz, and G. Beroza, Seismicity remotely triggered by the magnitude 7.3 Landers, California, earthquake, *Science*, *260*, 1617–1623, 1993.

Iio, Y., Slow initial phase of the p wave velocity pulse generated by microearthquakes, *Geophys. Res. Lett.*, *19*, 477–480, 1992.

Iio, Y., et al., Slow initial phase generated by microearthquakes occuring in the western Nagano prefecture, Japan, the source effect, *Geophys. Res. Lett.*, *126*, 1969–1972, 1999.

Ionescu, I., and M. Campillo, Influence of the shape of friction law and fault finiteness on the duration of initiation, *J. Geophys. Res.*, *104*, 3013–3024, 1999.

Kilb, D., J. Gomberg, and P. Bodin, Triggering of earthquake aftershocks by dynamic stresses, *Nature*, *408*, 570–574, 2000.

King, G., R. Stein, and J. Lin, Static stress changes and the triggering of earthquakes, *Bull. Seismol. Soc. Am.*, *84*, 935–953, 1994.

Lockner, D., and N. Beeler, Premonitory slip and tidal triggering of earthquakes, *J. Geophys. Res.*, *104*, 20,133–20,151, 1999.

Melchior, P., *The Tides of the Planet Earth*, Oxford Univ. Press, New York, 1983.

Ohnaka, M., Nonuniformity of the constitutive law parameters for shear rupture and quasistatic nucleation to dynamic rupture: A physical model

of earthquake generation processes, *Proc. Natl. Acad. Sci. USA*, *93*, 3795–3802, 1996.

Ohnaka, M., and T. Yamashita, A cohesive zone model for dynamic shear faulting based on experimentally inferred constitutive relation and strong motion source parameters, *J. Geophys. Res.*, *94*, 4089–4104, 1989.

Ohnaka, M., Y. Kuwahara, and K. Yamamoto, Constitutive relations between dynamic physical parameters near a tip of the propagating slip zone during stick-slip shear failure, *Tectonophysics*, *144*, 109–125, 1987.

Pulido, N., and K. Irikura, Estimation of dynamic rupture parameters from the radiated seismic energy and apparent stress, *Geophys. Res. Lett.*, *27*, 3945–3948, 2000.

Reinen, L., Seismic and aseismic slip indicators in serpentinite gouge, *Geology*, *28*, 135–138, 2000.

Simpson, R., S. Schulz, L. Dietz, and R. Burford, The response of creeping parts of the San Andreas Fault to earthquakes on nearby faults: Two examples, *Page Geophs.*, *126*, 665–685, 1988.

Smith, S., and W. Van de Lindt, Strain adjustments associated with earthquakes in southern California, *Bull. Seismol. Soc. Am.*, *59*, 1569–1589, 1969.

Stein, R., The role of stress transfer in earthquake occurrence, *Nature*, *402*, 605–609, 1999.

Vidale, J., D. Agnew, M. Johnston, and D. Oppenheimer, Absence of correlation with Earth tides: An indication of high preseismic fault stress rate, *J. Geophys. Res.*, *103*, 24,567–24,572, 1998.

Voisin, C., Dynamic triggering of earthquakes: The linear slip-dependent friction case, *Geophys. Res. Lett.*, *28*, 3357–3360, 2001.

Voisin, C., M. Campillo, I. Ionescu, F. Cotton, and O. Scotti, Dynamic versus static stress triggering and friction parameters: Inferences from the November 23, 1980, Irpinia earthquake, *J. Geophys. Res.*, *109*, 20,647–20,659, 2000.

Voisin, C., I. Ionescu, M. Campillo, R. Hassani, and Q. Nguyen, Process and signature of initiation on a finite fault system: A spectral approach, *Geophys. J. Int.*, *148*, 120–131, 2002.

Wright, T., E. Fielding, and B. Parsons, Triggered slip: Observations of the 17 August 1999 Izmit (Turkey) earthquake using radar interferometry, *Geophys. Res. Lett.*, *28*, 1079–1082, 2001.

Zhao, S., and S. Takemoto, Aseismic fault movement before the 1995 Kobe earthquake detected by a GPS survey: Implication for preseismic stress localization?, *Geophys. J. Int.*, *135*, 595–606, 1998.

C. Voisin, Laboratoire de Geophysique Interne de Tectonophysique, BP 53, 38041 Grenoble, France. (cvoisin@obs.ujf-grenoble.fr)